Structure of the microbial plankton community in the NW Iberian margin at the end of the upwelling season

B.G. Crespo[a,]*, O. Espinoza-González, I.G. Teixeira, C.G. Castro, F.G. Figueiras

Instituto de Investigacións Mariñas, CSIC, Eduardo Cabello 6, 36208 Vigo, Spain

[a] Present address: Departament de Biología i Oceanografía, Institut de Ciències del Mar, CSIC, 08003 Barcelona, Spain

*Corresponding author

E-mail address: bibiana@icm.csic.es

Phone: +34 932309500

Fax: +34 932309555

ABSTRACT

At the end of summer, seasonal upwelling at the NW Iberian Peninsula relaxes and nutrient depleted oceanic waters conveyed by the Iberian Poleward Current (IPC) converge on the western shelf with outwelled waters from the four bays known as Rías Baixas. At that time, with virtual absence of diatoms and dominance of nanoflagellates in the autotrophic microbial plankton community, *Synechococcus* accounted for ~ 20% of the total autotrophic biomass (AB). This situation contrasts with that previously reported for spring upwelling (Crespo et al., 2011), when diatoms were present in upwelled waters on the shelf and *Synechococcus* accounted for a minor fraction (0.16 ± 0.13%) of AB. Primary production (624 ± 585 mg C m^{-2} d^{-1}), 5-fold lower than in the spring upwelling, was particularly low (246 ± 104 mg C m^{-2} d^{-1}) at the IPC, though higher values (1616 ± 389 mg C m^{-2} d^{-1}) were measured on the western shelf in front of the Rías Baixas. Phytoplankton gross growth rates (μ) showed the same pattern of extremely low values in the IPC (μ = 0.06 d^{-1}) and the highest (μ = 0.27 d^{-1}) in the waters leaving the Rías Baixas. Whereas AB exceeded heterotrophic biomass (HB) in this upwelling system in spring, at the end of summer HB was higher than AB. However, both biomasses were linearly related with a HB:AB ratio of 1 and the excess of HB (intercept = 2.8 ± 0.5 g C m^{-2}) being similar to the rather constant bacterial biomass (2.7 ± 0.5 g C m^{-2}). This fact points to the key role played by bacteria during the oligotrophic conditions at the end of summer. Bacteria can maintain the functioning of the microbial community through processing dissolved organic matter and supplying food to heteretrophs and mixotrophs.

Keywords: Microbial community, nanoflagellates, *Synechococcus*, bacteria, heterotrophy, coastal upwelling, NW Iberian Peninsula

1. Introduction

It is well known that the size-structure and composition of the planktonic community influence the dynamics of the microbial food web and consequently biogeochemical cycles in the ocean (Azam et al., 1983). Although multiple stages of the microbial plankton community can be found in the sea, those commonly found in oligotrophic and eutrophic areas set the limits for all possible situations (Legendre and Rassoulzadegan, 1995). Picoplankton cells dominate in the microbial community of the oligotrophic ocean (Buck et al., 1996), where the microbial loop drives recycling (Azam et al., 1983). On the contrary, large plankton and export (Malone, 1980) characterise the structure and functioning of the microbial community in eutrophic areas.

According to this scheme, coastal upwelling systems should be classified as eutrophic areas because export and dominance of large cell-sized plankton are among the most obvious characteristics of these zones. However, coastal upwelling systems are essentially dynamic, with temporal and spatial variability modulating the structure and composition of the microbial community (Lorenzo et al., 2005; Sherr et al., 2005). Thus, picoplankton from the nearby oligotrophic ocean can be advected shoreward during downwelling, while intense upwelling can expand to the adjacent oligotrophic ocean the presence or dominance of large plankton. Coastline (bays and capes) and hydrographic singularities (eddies and fronts) can also modify the structure and composition of the microbial community through the changes they cause in upwelling and downwelling intensity (Figueiras et al., 2006; Crespo et al., 2011). The microbial community in eastern boundary upwelling ecosystems also experiences variability over the growth season, which is basically characterised by the continuous increase in the abundance of heterotrophs (Figueiras et al., 2002). Furthermore, in a changing world, with climate change altering the upwelling intensity and the extension of the upwelling

season (Álvarez-Salgado et al., 2008), it is reasonable to expect future changes in the structure and composition of the microbial community following changes in oceanographic conditions (Cermeño et al., 2008; Li et al., 2009; Morán et al., 2010). Therefore, knowledge of the structure and composition of the microbial community in these highly productive zones is not only important to understand the functioning of the microbial food web during the several upwelling-downwelling phases that these systems undergo, it is also relevant to track future modifications induced by environmental changes.

The NW Iberian Peninsula (Fig. 1a) constitutes the northern limit of the eastern boundary Large Marine Upwelling Ecosystem that extends from the African coast (10ºN) to the European coast (44ºN) (Wooster et al., 1976). Upwelling is seasonal at these latitudes (42-44 ºN), with northerly winds causing upwelling from spring to autumn and southerly winds inducing downwelling in winter (Wooster et al., 1976; Figueiras et al., 2002). Upwelling and downwelling force contrasting circulation patterns in the four bays located on the west of the NW Iberian Peninsula, collectively known as Rías Baixas (Fig. 1a). Upwelling induces positive estuary-like circulation in the Rías causing the export of material to the nearby shelf, whereas the reverse circulation occurs during downwelling, with shelf water entering the Rías (Figueiras et al., 2002).

The seasonal upwelling-downwelling transition at the end of summer coincides with the advection toward the coast of warm and saline oceanic water, which then flows northward on the slope forming the Iberian Poleward Current (IPC) (Haynes and Barton, 1990; Álvarez-Salgado et al., 2003; Torres and Barton, 2006). During this transition, with downwelling not totally established yet and upwelling relics still present in the region, a subsurface chlorophyll maximum (SCM) is typically observed in a well

stratified water column (Castro et al., 1997; Torres and Barton, 2006; Crespo et al., 2008). The microplankton community at the NW Iberian region during this transition time has been relatively well studied and now it is known that it is basically composed of small (~30 μm) dinoflagellates (Castro et al., 1997; Crespo et al., 2008), because downwelling precludes diatom growth and confines large dinoflagellates (>60 μm) inside the Rías (Fermín et al., 1996; Crespo et al., 2007). There is also some evidence pointing to the dominance of pico- and nanoplankton within the autotrophic community (Lorenzo et al., 2005; Rodríguez et al., 2006). In contrast, the trophic structure of the whole microbial community is relatively unknown.

Here we present a detailed analysis of the structure and composition of the autotrophic and heterotrophic microbial communities at the end of the upwelling season in this coastal upwelling region. The results, derived from data collected nearly 20 years ago (September 1991), are compared to those obtained from a contrasting upwelling situation in the spring of the same year (Crespo et al., 2011). This information is essential to understand the functioning of the pelagic system and develop an accurate plankton functional type (PTF) model for the region (Le Quéré et al., 2005) as a baseline to which future environmental changes can be referred.

2. Materials and methods

2.1. Sampling

The northwestern Iberian margin (Fig. 1a) was sampled at 37 stations located along 8 sections perpendicular to the shoreline at the end of the summer in 1991 (September 10 to 18). Starting at the northernmost section (Stns 11 to 14), sampling was carried out with a conductivity-temperature-depth (CTD) probe (SBE 9/11) equipped with a Sea Tech fluorometer and a rosette with 12 PVC Niskin bottles. Seawater samples were

collected from the CTD upcasts at several depths, between surface and bottom on the shelf and from surface to ~100 m at the other stations. To ensure that the SCM was sampled, the depths were selected after inspecting the fluorescence profiles. Nutrients and chlorophyll *a* (chl *a*) were determined at all sections, while the structure and composition of the microbial community were analysed at 18 stations situated along alternate sections (black symbols in Fig. 1a). Primary production was estimated from determinations of photosynthesis-irradiance relationships and light transmittance in the water column at 10 stations (triangles in Fig. 1a) randomly distributed on the sampling area. This distribution was due to the constraint imposed by sampling during day light hours. Seawater for photosynthesis-irradiance determinations was collected at 3-4 depths within the photic layer.

2.2. Ekman transport, nutrients and chl a

The cross-shelf Ekman transport (Fig. 1b) was estimated according to Bakun (1973) using geostrophic winds off Cape Finisterre (43ºN, 11º W).

Nitrate and ammonium concentrations (µmol kg^{-1}) were determined onboard by segmented flow analysis (Technicon AAII system) according to Hansen and Grasshoff (1983).

For chl *a* determinations 100 ml of seawater were filtered through 25 mm GF/F filters under low vacuum pressure. The filters were immediately frozen at -20ºC until pigment extraction in 90% acetone over 24 h in dark at 4ºC. Chl *a* concentrations (mg m^{-3}) were determined using a Turner Designs fluorometer calibrated with pure chl *a* (Sigma).

2.3. Microbial plankton biomass

Sub-samples of 10 ml were processed according to Porter and Feig (1980) to enumerate autotrophic and heterotrophic pico- (<2 µm) and nanoplankton (2-20 µm) by epifluorescence microscopy (see details in Figueiras et al., 2006). *Prochloroccoccus*, which can be found in shelf waters of the region at this time of the year (Rodríguez et al., 2006), were not well discriminated as autotrophs with this technique due to their low fluorescence. Thus, the abundance of picoautotrophs can be underestimated and the abundance of heterotrophic bacteria overestimated (Buck et al., 1996). Bacterial abundance was converted to carbon biomass according to Lee and Furhmann (1987). Dimensions were taken for the other groups and their biovolumes were calculated assuming a spherical shape. Cell carbon conversions were made according to Verity et al. (1992) for pico- and nanoflagellates and Bratbak and Dundas (1984) for *Synechococcus*.

Sub-samples of 100 ml preserved in Lugol´s iodine were settled in composite sedimentation chambers and examined with an inverted microscope to identify and count microplankton (20-200 µm) species of diatoms, dinoflagellates and ciliates. The small species were enumerated from two transects scanned at x250 and x400, whereas the less abundant larger species were counted from the whole slide scanned at x100. Epifluorescence microscopy and the list of species given by Lessard and Swift (1986) were used to differentiate between phototrophic and heterotrophic species. Dimensions were taken to estimate cell and plasma volumes by approximation to the nearest geometrical shape. The plasma volume of diatoms and the biovolume of dinoflagellates were converted to cell carbon following Strathmann (1967). Carbon biomass of ciliates was estimated according to Putt and Stoecker (1989).

2.4. Irradiance at the sea surface and in the water column

The photosynthetic active radiation (*PAR*, λ = 400-700 nm, µmol quanta m^{-2} s^{-1}) during the cruise was measured on deck with a Li-190SA cosine-sensor at 1 min intervals. These readings were then hourly integrated to obtain the daily distribution of incident irradiance at sea surface.

The *PAR* irradiance in the water column was measured at the 10 stations where primary production was determined. Readings were taken at 2 m intervals with a spherical quantum sensor LI-193SA. Incident irradiance at the sea surface (PAR_{0+}) was recorded at the same time with a cosine-sensor LI-190SA. Then, the *PAR* profile in the water column (PAR_z) was fitted to:

$$PAR_z = PAR_{0-}e^{-kz} \quad (1)$$

where k (m^{-1}) is the light attenuation coefficient and PAR_{0-} is the irradiance just below the sea surface. The ratio PAR_{0-}/PAR_{0+} provides the light transmittance at the air-sea interface.

2.5. Photosynthesis-irradiance relationships, primary production and phytoplankton growth rates

The photosynthesis-irradiance experiments were conducted in linear incubators (Arbones et al., 2000) illuminated on the front side with tungsten-halogen lamps (50W, 12 V) and refrigerated with circulating seawater. Each incubator housed 14 subsamples collected in 75 ml Corning tissue flasks, which were inoculated with 1.85 x 10^5 Bq (5 µCi) of ^{14}C-bicarbonate. One of these flasks was covered with aluminium foil and placed at the end of the incubator to check dark carbon fixation. Following incubation

(2 h), samples were filtered under low vacuum pressure through 25 mm GF/F filters that were then exposed to HCl fumes for 12 h to remove unincorporated inorganic ^{14}C. Radioactivity was measured with a liquid scintillation counter using the external standard and the channel ratio methods to correct for quenching.

In absence of photo-inhibition the data were fitted to the model of Webb et al. (1974):

$$P_z^B = P_m^B[1-\exp(-\alpha^B PAR/P_m^B)] \quad (2)$$

or to the model of Platt et al. (1980) when photo-inhibition was evident:

$$P_z^B = P_s^B[1-\exp(-\alpha^B PAR/P_s^B)]\exp(-\beta^B PAR/P_s^B) \quad (3)$$

to derive the chlorophyll-specific light saturated rate of photosynthesis (P_m^B , mg C mg chl a^{-1} h^{-1}), light saturated rate of photosynthesis in the absence of photo-inhibition (P_s^B , mg C mg chl a^{-1} h^{-1}), light-limited slopes (α^B , mg C mg chl a^{-1} h^{-1} (µmol quanta m^{-2} s^{-1})$^{-1}$) and coefficients of photo-inhibition (β^B , mg C mg chl a^{-1} h^{-1} (µmol quanta m^{-2} s^{-1})$^{-1}$). For the cases with photo-inhibition P_m^B was estimated when $\partial P^B/\partial PAR = 0$ (Platt et al., 1980). P_z^B is the chlorophyll-specific rate of carbon fixation (mg C mg chl a^{-1} h^{-1}) at each sampled depth.

The daily incident irradiance at sea surface and the vertical profiles of *PAR* and chl *a* concentration were combined in equations (2) and (3) to estimate the daily water-column primary production (PP, mg C m^{-2} d^{-1}) down to 1% of incident irradiance at sea surface. Integration was carried out at hourly steps and 1 m intervals.

Phytoplankton gross growth rate (μ, d^{-1}) was estimated at each sampled depth where carbon fixation was determined:

$$\mu = \ln\left(1 + \frac{dC/dt}{C_{ph}}\right) \quad (4)$$

where dC/dt is the volumetric carbon fixation (mg C m^{-3} d^{-1}) and C_{ph} is phytoplankton carbon (mg C m^{-3}).

3. Results and discussion

3.1. Meteorological and oceanographic conditions: the onset of the IPC

Northerly and southerly winds, coastal upwelling and coastal downwelling favourable respectively, alternated in the region in September 1991 (Fig. 1b). Thus, although the cruise began during strong downwelling (Q_x = -595 m^3 s^{-1} km^{-1}) on September 10th, the situation gradually reverted until the sampling ended under moderate upwelling on September 18th (Q_x = 270 m^3 s^{-1} km^{-1}). This is a wind regime commonly registered at the NW Iberian Peninsula during the seasonal upwelling-downwelling transition that leads to the onset of the IPC, while upwelling vestiges are still observed in the region (Castro et al., 1997; Álvarez-Salgado et al., 2003; Torres and Barton, 2006). The onset of the IPC regularly occurs with the advection of warm and saline oceanic surface water toward the west coast (Crespo and Figueiras, 2007; Relvas et al., 2007) as found during this study. Thus, warm (>20ºC; Fig. 2a) and saline (>35.7; Fig. 2b) waters observed at the most oceanic stations correspond to thermohaline properties characteristic of IPC advected waters. However, we observed no signal of these salty waters at the most northern sections, indicating that the IPC was not

completely developed. Therefore, we were capturing the onset of the IPC, as observed in detail by Haynes and Barton (1990) at the same time of the year. In fact, traces of upwelled waters with temperature <19º C were seen on the shelf at the northern locations (Fig. 2a). On the western shelf, the less saline waters (Fig. 2b) with high chlorophyll concentrations (Fig 2c) were exported from the Rías Baixas through their positive estuary-like circulation forced by upwelling (Figueiras et al. 2002; Crespo et al., 2007).

Although other effects may contribute, the wind-forced upwelling-downwelling response describes to first order the predominant dynamics over the NW Iberian shelf. Interactions with spatial inhomogeneity of the wind field and coastal orography (Torres et al., 2003) are detectable in the variability of the shelf regime, but are of secondary importance. Remote forcing of upwelling via coastally-trapped waves, although not observed in the region (e.g. Relvas et al., 2007) presumably must play a minor role. However, the direct wind response explains most of the variability observed in the NW Iberian upwelling system.

The whole region showed a strongly stratified water column (Figs. 3a-c) with a well-developed nitracline at ~50 m (Figs. 3d-f) to which a SCM was associated (Figs. 3g-i). The SCM, however, surfaced on the shelf (Figs. 3g-i) and this outcropping was reflected in the distribution of chl *a* concentration at sea surface (Fig. 2c), with higher values near the coast than in the IPC. Nevertheless, the chl *a* distribution recorded along the section situated in front of the Rías Baixas (Fig. 3i) points to the discontinuity between the SCM and the surface maximum nearest the coast. This suggests that phytoplankton exported from the Rías Baixas significantly contributed to the chl *a* maximum registered at stn 71 (Fig. 3i).

While nitrate was depleted in the upper water column (Figs. 3d-f), ammonium was relatively important at sea surface (Fig. 2d), with concentrations being particularly high (>1 µmol kg^{-1}) at the front separating IPC from shelf waters.

3.2. Autotrophic plankton biomass: the importance of picophytoplankton

The autotrophic community was largely dominated by autotrophic nanoflagellates (ANF), with significant contributions of *Synechococcus*, autotrophic picoflagellates (APF) and autotrophic dinoflagellates (AD) (Table 1). Diatoms and autotrophic ciliates (AC) accounted for a minor fraction (< 2%) of the total autotrophic biomass (AB). As the biomasses of these four dominant phytoplankton groups were linearly correlated ($r \geq 0.53$; $P < 0.001$; $n = 135$), spatial variations in AB (Figs. 4a-c) matched variations in the biomasses of these groups, mainly variations in ANF biomass (Figs.4d-f). However, there were small differences along the sections. Thus, the biomass of *Synechococcus* was higher near the coast at all sections sampled (Figs.4g-i; Table 1), whereas APF biomass was slightly higher in coastal waters at the northernmost section (Figs.4j-l; Table 1). ANF (Figs. 4d-f) and AD (Figs. 4m-o) showed highest biomass values in surface waters off the Rías Baixas (Stn 71; Figs 4f and o). Small species (*Heterocapsa niei*, *Prorocentrum minimum*) dominated in the AD community at all sites (Crespo et al., 2008), while the presence of large pigmented dinoflagellates (e.g. *Ceratium fusus*, *Prorocentrum micans*, *Dinophysis acuminata*) was restricted to surface waters of low salinity off the Rías Baixas (Crespo et al., 2008). These dinoflagellates were exported from the Rías to contribute to the maximum of biomass recorded at the surface of station 71 (Fig. 4o). It is also remarkable the low AB (<80 mg C m^{-3}) carried out by surface oceanic waters >20º C (Fig. 4). However, the presence of *Prochlorococcus* at the NW Iberian margin, which were not satisfactorily enumerated on this occasion, is

tightly coupled to the onset of the IPC (Rodríguez et al., 2006), and so it could be present in the warm and saline surface oceanic water advected to the region. Nevertheless, the NW Iberian Peninsula is near the northern limit of the distribution of *Prochlorococcus* in the Atlantic Ocean (Buck et al., 1996) and their abundance in IPC waters is always typically low ($<10^3$ cells ml^{-1}; Calvo-Díaz et al., 2004), around 2-3 fold lower than the abundance of *Synechococcus* recorded during this cruise in the surface waters of the IPC.

Despite this apparent coastal-ocean variability in the biomass of autotrophic plankton, the water-column integrated biomass values (Table 1) at coastal (the two most inshore stations) and oceanic stations were not significantly different ($P > 0.05$, t-test for two samples). This situation markedly contrasts with that found in the region during spring upwelling (Fig. 5), when a coastal environment with relatively low AB (8.7 ± 4.1 g C m^{-2}) and high contribution of diatoms (27 ± 17%) was clearly discernible from an oceanic environment with higher AB (24.5 ± 9.6 g C m^{-2}) and almost complete dominance of ANF (89 ± 6%). Another major difference between these two seasons refers to the importance of autotrophic picoplankton (*Synechococcus* and APF). Whereas in spring upwelling (Crespo et al., 2011) picophytoplankton represented a minor fraction of AB at both coastal and oceanic domains (2.3 ± 0.8%), especially evident for *Synechococcus* (0.2 ± 0.1%), their contribution at the end of summer (32 ± 9%) was appreciably higher (Table 1; Fig. 5). In addition, the biomass of autotrophic picoplankton at the end of summer (2.24 ± 0.88 g C m^{-2}) was substantially higher than in spring upwelling (0.42 ± 0.40 g C m^{-2}; Fig. 5), and this difference between the two seasons was particularly noticeable for *Synechococcus*, with an average biomass 35 times higher at the end of summer (1.41 ± 0.61 g C m^{-2}, Table 1) than in spring (0.04 ± 0.05 g C m^{-2}). In contrast, the biomass of ANF was lower and less variable at the end of

summer (3.69 ± 1.16 g C m^{-2}; Table 1) than in spring upwelling (12.99 ± 10.34 g C m^{-2}), when differences in ANF biomass between coastal and ocean domains were considerable (Fig. 5).

Higher biomass of autotrophic picoplankton in the rather oligotrophic waters at the end of summer than in the eutrophic conditions of spring, agrees well with similar situations described for other coastal upwelling systems (Sherr et al., 2005) and other coastal waters in general (Echevarría et al., 2009). It is also consistent with the macroecological pattern (Li, 2002) that describes an increase in autotrophic picoplankton abundance and a decrease in the abundance of larger cells following the degree of oligotrophy. In such a scenario, with dominance of nano- and picophytoplankton (Table 1), nitrate depletion (Figs. 3d-f) and relatively high concentrations of ammonium in the surface layer (Fig. 2d), considerable recycling within the microbial community and hence low f-ratios (Probyn, 1992) would be expected.

3.3. Carbon to chl a *ratio*

The distribution of AB (Figs. 4a-c) roughly followed that of chl *a* (Figs. 3g-i), according to a phytoplankton carbon to chl *a* (Cph:chl *a*) ratio of 170 ± 6 (Fig. 6). This relationship slightly improves to give a somewhat higher Cph:chl *a* ratio of 178 ± 5 when 6 points (3 from the northernmost section and other 3 points from the southernmost section) were removed from the regression. One of these points corresponds to a surface sample at the northernmost section with a high phytoplankton carbon value (305 mg C m^{-3}) and a relatively low chl *a* concentration (0.52 mg m^{-3}). The other 5 points belong to samples from the SCM (2 at the northernmost section and 3 at the southernmost section) with low Cph:chl *a* ratios (Fig. 6).

Ratios like this have been reported for oligotrophic areas in the open ocean (e.g. Buck et al., 1996) and they are commonly interpreted as a signal of nutrient limitation for phytoplankton growth (Marañón, 2005). However, high Cph:chl *a* ratios can also result from mixotrophic nutrition (Skovgaard et al., 2000), which is widespread within pigmented pico- (Zubkov and Tarran, 2008) and nanoplankton (Unrein et al., 2007). Therefore, mixotrophic nutrition at the NW Iberian margin under the oligotrophic conditions at the end of summer should not be disregarded. This is a nutrition mode that has also been suggested for pigmented nanoplankton in the region during spring (Crespo et al., 2011) to explain the high Cph:chl *a* found at the oceanic environment.

The existence of a unique Cph:chl *a* ratio for the whole area contrasts with the situation found during spring upwelling (Fig. 5), when near-shore waters with direct influence of upwelling showed a Cph:chl *a* ratio (38 ± 3) considerably lower than oceanic waters (157 ± 8). The occurrence of a unique ratio, without differences between surface and SCM, also suggests that photo-acclimation in the SCM was not important, which in turn points to the recent formation of the SCM. Then, the SCM formation probably occurred through the subduction of coastal surface waters forced by the advection of surface oceanic water with low chl *a* concentration (Fig. 2c) and low phytoplankton biomass (Fig. 4). If this is the process responsible for the formation of the SCM, the corollary is that the phytoplankton populations, including picophytoplankton, found in the area were not transported from the open ocean. On the contrary, picophytoplankton must be viewed as a typical component of the phytoplankton community in coastal upwelling systems that get more importance under non upwelling conditions (Lorenzo et al., 2005; Sherr et al., 2005).

3.4. Primary production and phytoplankton growth

Primary production (Table 2), was highly variable (624 ± 585 mg C m^{-2} d^{-1}), with the lowest value (128 mg C m^{-2} d^{-1}) occurring in the IPC waters at the southwest corner (stn 85; Fig 1a) and the highest (1891 mg C m^{-2} d^{-1}) in waters leaving the shelf at 42.5 ºN (stn 65, Fig. 1a). The low PP (246 ± 104 mg C m^{-2} d^{-1}) measured in the IPC (Table 2) is typical of oligotrophic waters (Frazel and Berberian, 1990; Lorenzo et al. 2004) and was similar to values previously reported for the IPC at the NW Iberian Peninsula (Tilstone et al., 2003), when microbial community respiration exceeds carbon fixation (Teira et al., 2001). Primary production in western shelf waters (1616 ± 389 mg Cm^{-2} d^{-1}) lies within the range of values reported for stratified or not strong upwelling conditions on the shelf (Tilstone et al., 2003; Lorenzo et al., 2005). However, it was appreciably lower than the values commonly measured during upwelling (Teira et al., 2001; Tilstone et al., 2003). The PP determined at the northern shelf not affected by the IPC (593 ± 319 mg C m^{-2} d^{-1}) can be considered as representative of summer stratified conditions (Teira et al., 2001; Tilstone et al., 2003), when the microbial community tends to be in metabolic balance (Teira et al., 2001). Overall, PP during this cruise at the end of summer was 5-fold lower than PP measured during spring upwelling in the same area (Fig. 5).

Although phytoplankton gross growth rates were generally higher at sea surface (0.17 ± 0.10 d^{-1}) than at SCM (0.06 ± 0.04 d^{-1}), they were extremely low in the whole photic layer. As the rates estimated using Cph actually determined (equation 4) were not significantly different (P = 0.61; t-test for paired samples) to the rates estimated with Cph derived from the Cph:chl *a* ratio of 170 (Fig. 6), the mean gross growth rates ($\overline{\mu}$, d^{-1}) in the photic layer ($Z_{1\%}$) were estimated as:

$$\overline{\mu} = \frac{1}{Z_{1\%}} \int_{Z1\%} \ln\left(1 + \frac{dC/dt}{C_{ph}}\right) \quad (5)$$

where Cph was derived from the profiles of chl *a* concentration at each station where PP was measured.

The resulting gross growth rates varied from a minimum value of 0.06 d^{-1} at stn 72 in the IPC to a maximum value of 0.27 d^{-1} in the shelf waters in front of the Rías (stn 63), and they are similar to the gross growth rates recorded in the oceanic domain in spring (Fig. 5), where mixotrophic nutrition was presumably high (Crespo et al., 2011). These low rates, which correspond to doubling times of the phytoplankton community varying between 11.25 and 2.54 days (Table 2), are within the range of values found in the oligotrophic waters of subtropical gyres (Marañón, 2005) where nutrient limitation of phytoplankton growth is assumed. However, it must be noted that these gross growth rates were estimated for photosynthetic carbon fixation, and consequently they could be lower than the achieved rates if mixotrophic nutrition of ANF and APF occurs.

3.5. Microbial heterotrophic biomass and heterotrophic to autotrophic biomass ratio

The heterotrophic community was dominated by heterotrophic nanoflagellates (HNF) and bacteria (Table 3), with the two groups accounting for 77 ± 10% of the total integrated heterotrophic biomass (HB). Heterotrophic picoflagellates (HPF) and heterotrophic dinoflagellates (HD) also showed an appreciably contribution (~ 10%) to HB (Table 3). Unlike the strong reduction (57%) experienced by AB when compared to the AB registered in the region during spring upwelling, the drop in HB (22%) was substantially lower (Fig. 5). This leads to a system in which HB exceeded AB, in agreement with the expected situation for low nutrient conditions (Duarte et al., 2000),

with heterotrophic metabolism predominating in the microbial community (Teira et al., 2001). The reduction in HB occurred through the strong decrease (56%) in the HNF biomass (Table 3; Fig. 5), because bacterial biomass remained invariant (Table 3; Fig. 5) and the biomass of the other heterotrophic groups increased.

Although the distribution of HD (Figs. 7m-o) and heterotrophic ciliates (data not shown) show a preference of these two groups for coastal waters, the distributions of the other groups (Figs. 7d-l) as well as that of HB (Figs. 7a-c) were basically similar to the distributions of autotrophic plankton (Fig. 4). In fact, both HB and AB covaried (Fig. 8) according to a linear relationship with slope of 1, which suggests a rapid response of heterotrophic plankton to variations in the autotrophic components of the microbial community. On other hand, the intercept of this relationship (~30 mg C m^{-3}) that accounts for the excess of HB recorded in the system (Tables 1 and 3), roughly coincides with the average biomass of bacteria in a water column 100 m depth (Table 3). This constant biomass indicates that there is top-down control of bacteria and they can be viewed as playing a pivotal role at the NW Iberian margin under the oligotrophic conditions at the end of summer. Bacteria, through processing the dissolved organic matter, mainly exported from the Rías, and accumulated in the upper water column over the growth season (Álvarez-Salgado et al., 1999), can supply food to other heterotrophs and mixotrophs.

4. Summary

The microbial plankton community in the NW Iberian margin at the end of the upwelling season appeared dominated by heterotrophs, with nano- and picoplankton cells prevailing in both the autotrophic and heterotrophic community. This composition of the microbial community seems to be characteristic of the system, rather than being

advected from the adjacent oligotrophic ocean by downwelling. It markedly contrasts with the structure and composition of the microbial community recorded during spring upwelling, which was characterised by the dominance of autotrophs with presence of diatoms in a near-shore band directly affected by upwelling (Crespo et al., 2011). The high Cph: chl *a* ratios, the low primary production and the extremely low phytoplankton growth rates recorded at the end of the upwelling season points to a microbial community with predominance of heterotrophic processes, as the excess of heterotrophic biomass and the tight coupling of variations in autotrophic and heterotrophic biomasses suggest. The relatively constant bacterial biomass, which roughly matches the excess of heterotrophic biomass recorded in the system, points to the key role played by bacteria at the NW Iberian upwelling during the regularly observed oligotrophic conditions at the end of summer. In this context, bacteria can maintain the microbial community functioning through processing the dissolved organic matter accumulated over the upwelling season and so supplying food to heterotrophs and mixotrophs. Under a possible future scenario with lower upwelling intensity and shorter upwelling season in the region (Álvarez-Salgado et al., 2008), the structure and composition of the microbial community reported here, with heterotrophy dominating in the upper layer, will prevail in the zone. In the actual regime, the export from the Rías could supply the organic matter needed to maintain the functioning of the microbial community. However, with possible decreases in upwelling intensity and shortness of the upwelling season, the microbial community of the Rías Baixas, now predominantly autotrophic (Arbones et al., 2008), could eventually shift to heterotrophy leading to oligotrophy in the entire NW Iberian margin.

Acknowledgements

We thank the members of the Oceanography group at the Instituto de Investigacións Mariñas who participated in the cruise. Special thanks to E.D. Barton, for suggestions to improve the description of the physical field. This work was funded by the EU project MAST-CT90-0017 “The control of phytoplankton dominance” and by the Spanish project CTM2007-66408-C02-01/MAR (Ministerio de Educación y Ciencia). B.G.C. was supported by a Xunta de Galicia *Ángeles Alvariño* fellowship and the Stanley W. Watson Chair for Excellence in Oceanography under a Postdoctoral program at the Woods Hole Oceanographic Institution. O.E.G was supported by a *Mideplan* fellowship from the government of Chile.

References

Álvarez-Salgado, X.A., Doval, M.D., Pérez, F.F., 1999. Dissolved organic matter in shelf waters off the Ría de Vigo (NW Iberian upwelling system). J. Mar. Syst. 18, 383-394.

Álvarez-Salgado, X.A., Figueiras, F.G., Pérez, F.F., Groom, S., Nogueira, E., Borges, A.V., Chou, L., Castro, C.G., Moncoiffé, G., Ríos, A.F., Miller, A.E.J., Frankignoulle, M., Savidge, G., Wollast, R., 2003. The Portugal coastal counter current off NW Spain: new insights on its biogeochemical variability. Progr. Oceanogr. 56, 281-321.

Álvarez-Salgado, X.A., Labarta, U., Fernández-Reiriz, M.J., Figueiras, F.G., Rosón, G., Piedracoba, S., Filgueira, R., Cabanas, J.M., 2008. Renewal time and the impact of harmful algal blooms on the extensive mussel raft culture of the Iberian coastal upwelling system (SW Europe). Harmful Algae 7, 849-855.

Arbones, B., Castro, C.G., Alonso-Pérez, F., Figueiras, F.G., 2008. Phytoplankton size structure and water column metabolic balance in a coastal upwelling system: the Ría de Vigo, NW Iberia. Aquat. Microb. Ecol. 50, 169-179.

Arbones, B., Figueiras, F.G., Varela, R., 2000. Action spectrum and maximum quantum yield of carbon fixation in natural phytoplankton populations: implications for primary production estimates in the ocean. J. Mar. Syst. 26, 97-114.

Azam, F., Fenchel, T., Field, J.G., Gray, J.S., Meyer-Reil, L.A., Thingstad, F., 1983. The ecological role of water-column microbes in the sea. Mar. Ecol. Progr. Ser. 10, 257-263.

Bakun, A., 1973. Coastal upwelling indices, west coast of North America 1946-1971. NOAA technical report, NMFSSSRF-671, 103 pp.

Bratbak. G., Dundas, I., 1984. Bacterial dry matter content and biomass estimation. Appl. Environ. Microb. 48, 755-757.

Buck, K.R., Chavez, F.P., Campbell, L., 1996. Basin-wide distributions of living carbon components and the inverted trophic pyramid of the central gyre of the North Atlantic Ocean, summer 1993. Aquat. Microb. Ecol. 10, 283-298.

Calvo-Díaz, A., Morán, X.A.G., Nogueira, E., Bode, A., Varela, M., 2004. Picoplankton community structure along the northern Iberian continental margin in late winter-early spring. J. Plankt. Res. 26, 1069-1081.

Castro, C.G., Álvarez-Salgado, X.A., Figueiras, F.G., Pérez, F.F., Fraga, F., 1997. Transient hydrographic and chemical conditions affecting microplankton populations in the coastal transtion zone of The Iberian upwelling system (NW Spain) in September 1986. J. Mar. Res. 55, 321-352.

Cermeño, P., Dutkiewicz, S., Harris, R.P., Follows, M., Schofield, O., Falkowski, P.G., 2008. The role of nutricline depth in regulating the ocean carbon cycle. Proc. Nati. Acad. Sci. USA 105, 20344-20349.

Crespo, B.G., Espinoza-González, O., Teixeira, I.G., Castro, C.G., Figueiras, F.G., 2011. Possible mixotrophy of pigmented nanoflagellates: Microbial plankton biomass, primary production and phytoplankton growth at the NW Iberian upwelling in spring. Estuar. Coast. Shelf Sci. 94, 172-181.

Crespo, B.G., Figueiras, F.G., 2007. A spring poleward current and its influence on microplankton assemblages and harmful dinoflagellates on the western Iberian coast. Harmful Algae 6, 686-699.

Crespo, B.G., Figueiras, F.G., Groom, S., 2007. Role of across-shelf currents in the dynamics of harmful dinoflagellate blooms in the northwestern Iberian upwelling. Limnol. Oceanogr. 52, 2668-2678.

Crespo, B.G., Teixeira, I.G., Figueiras, F.G., Castro, C.G., 2008. Microplankton composition off NW Iberia at the end of the upwelling season: source areas of harmful dinoflagellate blooms. Mar. Ecol. Progr. Ser. 355, 31-43.

Duarte, C.M., Agustí, S., Gasol, J.M., Vaqué, D., Vazquez-Dominguez, E., 2000. Effect of nutrient supply on the biomass structure of planktonic communities: an experimental test on a Mediterranean coastal community. Mar. Ecol. Prog. Ser. 206, 87-95.

Echevarría, F., Zabala, L., Corzo, A., Navarro, G., Prieto, L., Macías, D., 2009. Spatial distribution of autotrophic picoplankton in relation to physical forcings: the Gulf of Cádiz, Strait of Gibraltar and Alborán Sea case study. J. Plankt. Res. 31, 1339-1351.

Fermín, E.G., Figueiras, F.G., Arbones, B., Villarino, M.L., 1996. Short-time scale development of a *Gymnodinium catenatum* population in the Ría de Vigo (NW Spain). J. Phycol. 32, 212-221.

Figueiras, F.G., Labarta, U., Fernádez Reíriz, M.J., 2002. Coastal upwelling, primary production and mussel growth in the Rías Baixas of Galicia. Hydrobiologia 484, 121-131.

Figueiras, F.G., Zdanowski, M.K., Crespo, B.G., 2006. Spatial variability in bacterial abundance and other microbial components in the NW Iberian margin during relaxation of a spring upwelling event. Aquat. Microb. Ecol. 43, 255-266.

Frazel, D.W., Berberian, G., 1990. Distributions of chlorophyll and primary productivity in relation to water column structure in the eastern North Atlantic Ocean. Glob. Biogeochem. Cycles 4, 241-251.

Hansen, H.P., Grasshoff, K., 1983. Automated chemical analysis, in: Grasshoff, K., Ehrhardt, M., Kremling, K. (Eds.), Methods of Seawater Analysis. Verlag Chemie Weinheime, pp. 347-379.

Haynes, R., Barton, E.D., 1990. A poleward flow along the Atlantic coast of the Iberian Peninsula. J. Geophys. Res. 95, 11425-11442.

Lee, S., Fuhrmann, J.A., 1987. Relationships between biovolume and biomass of naturally derived marine bacterioplankton. Appl. Environ. Microb. 53, 1298-1303.

Legendre, L., Rassoulzadegan, F., 1995. Plankton and nutrient dynamics in marine waters. Ophelia 41, 153-172.

Le Quéré, C., Harrison, S.P., Prentice, I.C., Buitenhuis, E.T., Aumont, O., Bopp, L., Claustre, H., Da Cunha, L.C., Geider, R., Giraud, X., Klaas, C., Kohfeld, K.E., Legendre, L., Manizza, M., Platt, T., Rivkin, R., Sathyendranath, S., Uitz, J., Warson, A.J., Wolf-Gladrow, D., 2005. Ecosystem dynamics based on plankton functional types for global ocean biogeochemistry models. Global Change Biology 11, 2016-2040.

Lessard, E.J., Swift, E., 1986. Dinoflagellates from the North Atlantic classified as phototrophic or heterotrophic by epifluorescence microscopy. J. Plankton Res. 8, 1209-1215.

Li, W.K.W., 2002. Macroecological patterns of phytoplankton in the northwestern North Atlantic Ocean. Nature 41-, 154-157.

Li, W.K.W., NcLaughlin, F.A., Lovejoy, C., Carmarck, E.C., 2009. Smallest algae thrive as the Artic Ocean freshens. Science 326, 539.

Lorenzo, L.M., Arbones, B., Tilstone, G.H., Figueiras, F.G. 2005. Across-shelf variability of phytoplankton composition, photosynthetic parameters and primary production in the NW Iberian upwelling system. J. Mar. Syst. 54, 157-173.

Lorenzo, L.M., Figueiras, F.G., Tilstone, G.H., Arbones, B., Mirón, I., 2004. Photosynthesis and light regime in the Azores Front region during summer: are light-saturated computations of primary production sufficient? Deep-Sea Res. I 51, 1229-1244.

Malone, T.C., 1980. Algal size, in: Morris, I. (Ed), The physiological ecology of phytoplankton. Univ. of Calif., Berkeley, pp. 433-463.

Marañón, E., 2005. Phytoplankton growth rates in the Atlantic subtropical gyres. Limnol. Oceanogr. 50, 299-310.

Morán, X.A.G., López-Urrutia, A., Calvo-Díaz, A., Li, W.K.W., 2010. Increasing importance of small phytoplankton in a warmer ocean. Glob. Change Biol. 16, 1137-1144.

Platt, T., Gallegos, C.L., Harrison, W.G., 1980. Photoinhibition of photosynthesis in natural assemblages of marine phytoplankton. J. Mar. Res. 38, 687-701.

Porter, K.G., Feig, Y.S., 1980. The use of DAPI for identifying and counting aquatic microflora. Limnol. Oceanogr. 25, 943-948.

Probyn, T.A., 1992. The inorganic nitrogen nutrition of phytoplankton in the Southern Benguela: new production, phytoplankton size and implications for pelagic foodwebs. S. Afr. J. Mar. Sci. 12, 411-420.

Putt, M., Stoecker, D.K., 1989. An experimental determined carbon:volume ratio for marine "oligotrichous" ciliates from estuarine and coastal waters. Limnol. Oceanogr. 34, 1097-1103.

Relvas, P., Barton, E.D., Dubert, J., Oliveira, P.B., Peliz, A., da Silva, J.C.B., Santos, A.M.P. 2007. Physical oceanography of the western Iberia ecosystem: Latest views and challenges. Progr. Oceanogr. 74, 149-173.

Rodríguez, F., Garrido, J.L., Crespo, B.G., Arbones, B., Figueiras, F.G., 2006. Size-fractionated phytoplankton pigment groups in the NW Iberian upwelling system: impact of the Iberian Poleward Current. Mar. Ecol. Prog. Ser. 232, 59-73.

Sherr, E.B., Sherr, B.F., Wheeler, P.A., 2005. Distribution of coccoid cyanobacteria and small eukaryotic phytoplankton in the upwelling ecosystem off Oregon coast during 2001 and 2002. Deep-Sea Res. II 52, 317-330.

Skovgaard, A., Hansen, P.J., Stoecker, D.K., 2000. Physiology of the mixotrophic dinoflagellate *Fragilidium subglobosum*. I. Effects of phagotrophy and irradiance on photosynthesis and carbon content. Mar. Ecol. Prog. Ser. 201, 129-136.

Strathmann, R., 1967. Estimating the organic carbon content of phytoplankton from cell volume or plasma volume. Limnol. Oceanogr. 12, 411-418.

Teira, E., Serret, P., Fernández, E., 2001. Phytoplankton size-structure, particulate and dissolved organic carbon production and oxygen fluxes through microbial communities in the NW Iberian coastal transition zone. Mar. Ecol. Prog. Ser. 219, 65-83.

Tilstone, G.H., Figueiras, F.G., Lorenzo, L.M., Arbones, B., 2003. Phytoplankton composition, photosynthesis and primary production during different hydrographic conditions at the Northwest Iberian upwelling system. Mar. Ecol. Prog. Ser. 252, 89-104.

Torres, R., Barton, E.D., 2006. Onset and development of the Iberian poleward flow along the Galician coast. Cont. Shelf. Res. 26, 1134-1153.

Torres, R., Barton, E.D., Miller, P., Fanjul, E. 2003. Spatial patterns of wind and sea surface temperature in the Galician upwelling region, J. Geophys. Res. 108(C4), 3130, doi:10.1029/2002JC001361.

Unrein, F., Massana, R., Alonso-Sáez, L., Gasol, J.M., 2007. Significant year-round effect of small mixotrophic flagellates on bacterioplankton in an oligotrophic coastal system. Limnol. Oceanogr. 52, 456-469.

Verity, P.G., Robertson, C.Y., Tronzo, C.R., Andrews, M.G., Nelson, J.R., Sieracki, M.E., 1992. Relationships between cell volume and the carbon and nitrogen content of marine photosynthetic nanoplankton. Limnol. Oceanogr. 37, 1434-1446.

Webb, W.L., Newton, M., Starr, D., 1974. Carbon dioxide exchange of *Alnus rubra*: a mathematical model. Oecologia 17, 281-291.

Woster, W.S., Bakun, A., McLain, D.R., 1976. The seasonal upwelling cycle along the eastern boundary of. The North Atlantic. J. Mar. Res. 34,131-141.

Zubkov, M.V., Tarran, G.A., 2008. High bacterivory by the smallest phytoplankton in the North Atlantic Ocean. Nature 455, 224-226.

Figure legends

Fig. 1. (a) The NW Iberian margin showing the location of the four Rías Baixas on the west coast and the stations sampled. The sections selected for vertical representations in Figs. 3, 4 and 7 are marked with black lines. Black symbols denote the stations where the structure and composition of the microbial plankton community were determined. The ten stations where primary production and phytoplankton growth rates were estimated are marked with black and open triangles. (b) Cross-shore Ekman transport component (-Qx) from September 1 to 20, 1991, estimated at 43º N, 11º W. Positive/negative values of –Qx indicate offshore/onshore transport (upwelling/downwelling) of surface waters.

Fig. 2. Sea surface distributions of (a) temperature, (b) salinity, (c) chl *a* concentration and (d) ammonium concentration.

Fig. 3. Vertical distributions at 3 selected sections (see Fig. 1a) of (a to c) temperature, (d to f) nitrate concentration and (g to i) chl *a* concentration. Section 11 to 14 was sampled on 10th September, section 51 to 55 on 13th September and section 71 to 75 on 16th September.

Fig. 4. Vertical distributions at 3 selected sections (see Fig. 1a) of (a to c) total autotrophic biomass (AB), (d to f) biomass of autotrophic nanoflagellates (ANF), (g to i) biomass of *Synechococcus* (SYN), (j to l) biomass of autotrophic picoflagellates (APF) and (m to o) biomass of autotrophic dinoflagellates (AD). Dashed line corresponds to the isotherm of 20º C at the oceanic stations (see Fig. 2a). Section 11 to 14 was sampled on 10th September, section 51 to 55 on 13th September and section 71 to 75 on 16th September.

Fig. 5. Cartoon summarising the contrasting structures of the microbial plankton community found in the NW Iberian upwelling at the end of summer (this work) and in spring upwelling (Crespo et al., 2011), when two domains (coastal and oceanic) were evident. The total area of the circles, as well as the areas of the portions representing the different plankton groups in each circle, is proportional to the respective biomass values. In the upper panel, representing the autotrophic community, the average value for phytoplankton carbon to chlorophyll *a* ratios (Cph:chl a), integrated primary production (PP) and phytoplankton growth rates estimated from carbon fixation (μ) are also given. Syn: *Synechococcus*; APF: autotrophic picoflagellates; ANF: autotrophic nanoflagellates; Diat: diatoms; AD: autotrophic dinoflagellates; AC : autotrophic ciliates. The heterotrophic community, with lesser variability than the autotrophic community, is represented in the lower panel. HPF: heterotrophic picoflagellates; HNF: heterotrophic nanoflagellates; HD: heterotrophic dinoflagellates; HC: heterotrophic ciliates.

Fig. 6. Phytoplankton carbon (Cph) to chl *a* relationships including all samples (solid line) Cph = (170 ± 6) chl *a*, $r^2 = 0.68$, n = 135; and removing 6 samples (open circles) from the regression (dashed line) Cph = (178 ± 5) chl *a*, $r^2 = 0.79$. See text for more details.

Fig. 7. Vertical distributions at 3 selected sections (see Fig. 1a) of (a to c) total heterotrophic biomass (HB), (d to f) biomass of heterotrophic nanoflagellates (HNF), (g to i) biomass of heterotrophic bacteria, (j to l) biomass of heterotrophic picoflagellates (HPF) and (m to o) biomass of heterotrophic dinoflagellates (HD). Dashed line corresponds to the isotherm of 20º C at the oceanic stations (see Fig. 2a). Section 11 to 14 was sampled on 10th September, section 51 to 55 on 13th September and section 71 to 75 on 16th September.

Fig. 8. Autotrophic biomass (AB) *versus* heterotrophic biomass (HB). Solid line, HB = (28.17 ± 5.40) + (1.02 ± 0.05)AB, $r^2 = 0.73$, n = 135, defines the relationship considering all points, which is not markedly different from the relationships obtained after excluding 3 samples (open circles, dashed line), HB = (30.15 ± 3.06) + (0.97 ± 0.03)AB, $r^2 = 0.90$.

Table 1. Integrated (surface-bottom on the shelf and 0-100 m at the ocean) values of chl *a* concentration (mg m^{-2}) and autotrophic plankton biomass (g C m^{-2}) at each station sampled. AB: total autotrophic biomass; *Syn*: *Synechococcus*; APF: autotrophic picoflagellates; ANF: autotrophic nanoflagellates; Diat: diatoms; AD: autotrophic dinoflagellates; AC: autotrophic ciliates. Average values and contribution of each group to AB are also given.

Stn	chl *a*	AB	*Syn*	APF	ANF	Diat	AD	AC
11	45	6.79	1.60	1.78	2.71	0.03	0.52	0.15
12	24	4.31	0.77	0.39	1.79	0.03	1.32	0.02
13	22	6.81	0.75	0.28	4.94	0.02	0.81	0.01
14	29	5.00	0.70	0.30	3.19	0.05	0.75	0.00
31	34	6.86	1.12	0.76	4.25	0.09	0.58	0.06
32	52	10.38	2.12	1.35	6.17	0.05	0.64	0.06
33	41	6.97	2.18	0.95	3.07	0.02	0.74	0.01
34	32	5.61	1.14	0.59	3.24	0.07	0.55	0.02
51	42	6.36	1.46	0.83	2.83	0.26	0.42	0.56
52	48	8.25	2.51	1.02	3.21	0.02	1.05	0.43
53	39	7.89	2.00	0.74	3.91	0.02	1.02	0.19
54	39	6.89	1.12	0.62	4.31	0.02	0.75	0.06
55	41	6.37	0.91	0.67	4.16	0.03	0.59	0.01
71	67	10.89	1.52	0.86	5.68	0.84	1.89	0.09
72	32	7.87	2.20	0.96	3.64	0.02	1.00	0.05
73	36	8.98	1.83	1.18	4.49	0.04	1.42	0.02
74	43	4.79	0.74	0.96	2.34	0.02	0.71	0.02
75	35	4.96	0.63	0.85	2.53	0.02	0.91	0.01
Average (SD)	39 (11)	7.00 (1.83)	1.41 (0.61)	0.84 (0.37)	3.69 (1.16)	0.09 (0.19)	0.87 (0.37)	0.10 (0.16)
Percentage of AB (SD)			19.7 (6.1)	12.1 (5.1)	52.8 (9.8)	1.1 (1.9)	12.9 (5.7)	1.4 (2.3)

Table 2. Primary production (PP, mg C m^{-2} d^{-1}), mean phytoplankton growth rate in the photic layer ($\overline{\mu}$, d^{-1}) and doubling time (1/k, days) in the 3 hydrographic zones identified at the end of summer in the NW Iberian margin. k = ln(2)/$\overline{\mu}$.

Zone	Stn	PP	$\overline{\mu}$	1/k
North	12	225	0.10	7.25
	14	770	0.15	4.63
	24	783	0.20	3.45
IPC	34	365	0.11	6.13
	44	345	0.23	3.04
	55	215	0.10	7.08
	72	177	0.06	11.25
	85	128	0.13	5.22
West-Rías	63	1341	0.27	2.54
	65	1891	0.22	3.21

Table 3. Integrated (surface-bottom on the shelf and 0-100 m at the ocean) values of microbial heterotrophic plankton biomass (g C m^{-2}) at each station sampled. HB: total heterotrophic biomass; HPF: heterotrophic picoflagellates; HNF: heterotrophic nanoflagellates; HD: heterotrophic dinoflagellates; HC: heterotrophic ciliates. Average values and contribution of each group to HB are also given.

Stn	HB	Bacteria	HPF	HNF	HD	HC
11	13.03	3.10	1.90	3.36	4.07	0.60
12	10.91	2.41	0.95	3.50	3.75	0.30
13	9.21	2.20	0.89	5.19	0.84	0.09
14	7.58	2.02	0.60	4.28	0.48	0.20
31	9.30	2.05	0.81	5.18	0.66	0.61
32	12.40	3.01	1.28	7.11	0.30	0.70
33	8.56	2.76	1.09	4.31	0.22	0.19
34	7.79	2.65	0.82	3.74	0.39	0.19
51	8.35	2.26	0.79	3.47	1.53	0.31
52	9.48	3.48	0.99	4.12	0.50	0.40
53	10.37	3.02	0.74	5.07	1.05	0.49
54	9.60	2.66	0.85	5.31	0.47	0.30
55	9.21	2.30	0.96	5.53	0.35	0.06
71	12.80	3.45	1.07	7.00	1.01	0.27
72	10.90	3.21	1.25	5.03	1.15	0.27
73	10.92	2.95	1.26	6.25	0.13	0.33
74	7.98	2.46	1.21	3.92	0.12	0.27
75	7.06	2.09	1.03	3.56	0.10	0.28
Average (SD)	9.75 (1.79)	2.67 (0.48)	1.03 (0.29)	4.77 (1.17)	0.95 (1.15)	0.32 (0.17)
Percentage of HB (SD)		27.7 (4.0)	10.6 (2.4)	49.4 (9.1)	9.1 (9.6)	3.3 (1.5)

Figure1
Click here to download Figure(s): Fig1.pdf

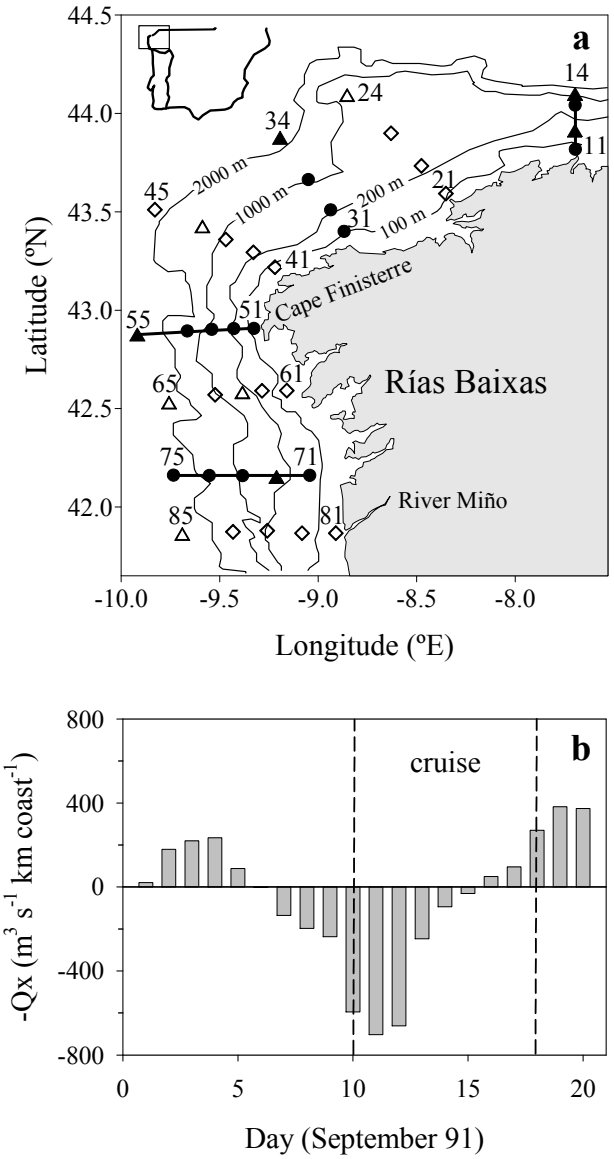

Fig. 1
Crespo et al.

Figure2
Click here to download Figure(s): Fig2.pdf

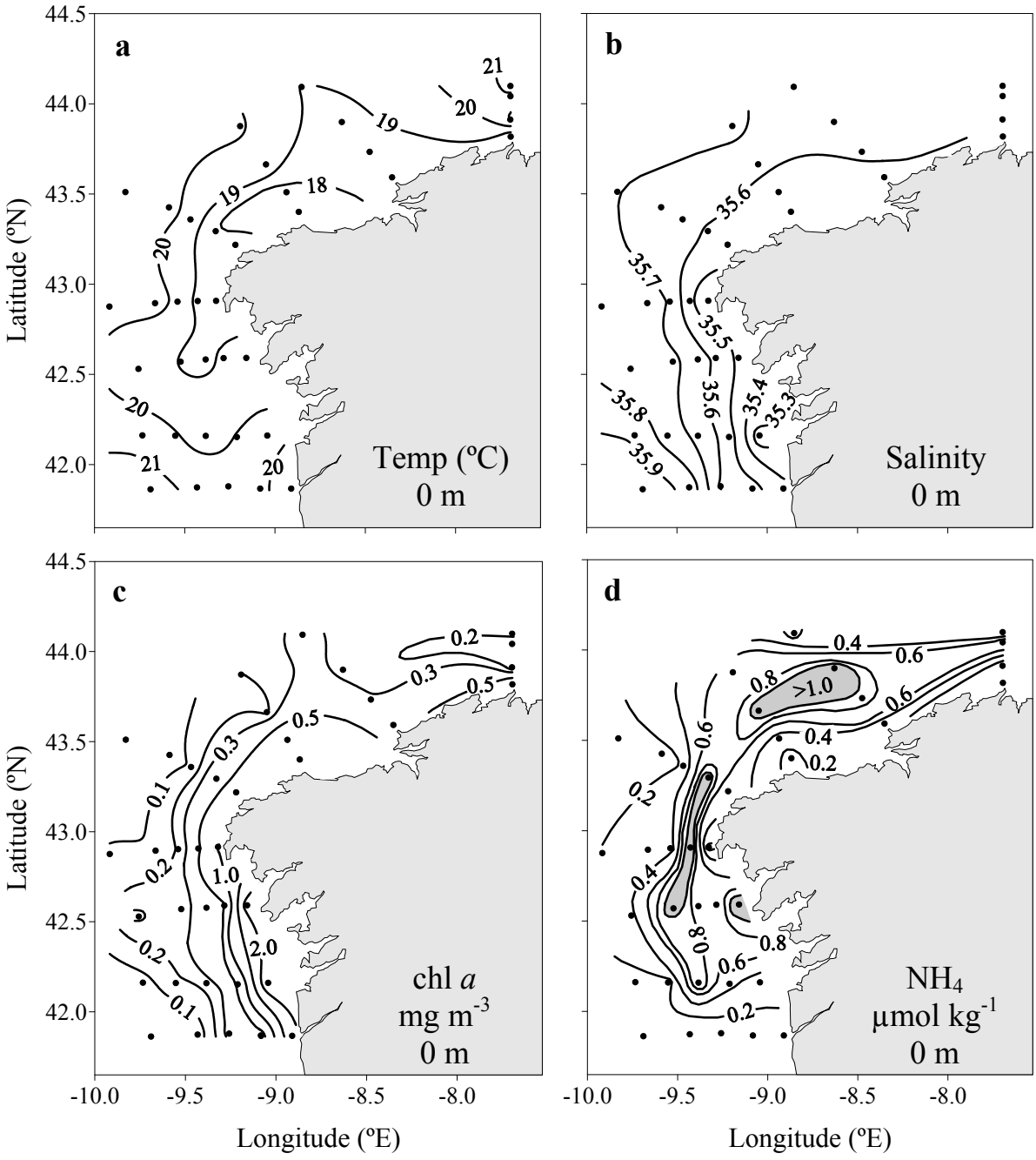

Fig. 2
Crespo et al.

Figure3
Click here to download Figure(s): Fig3.pdf

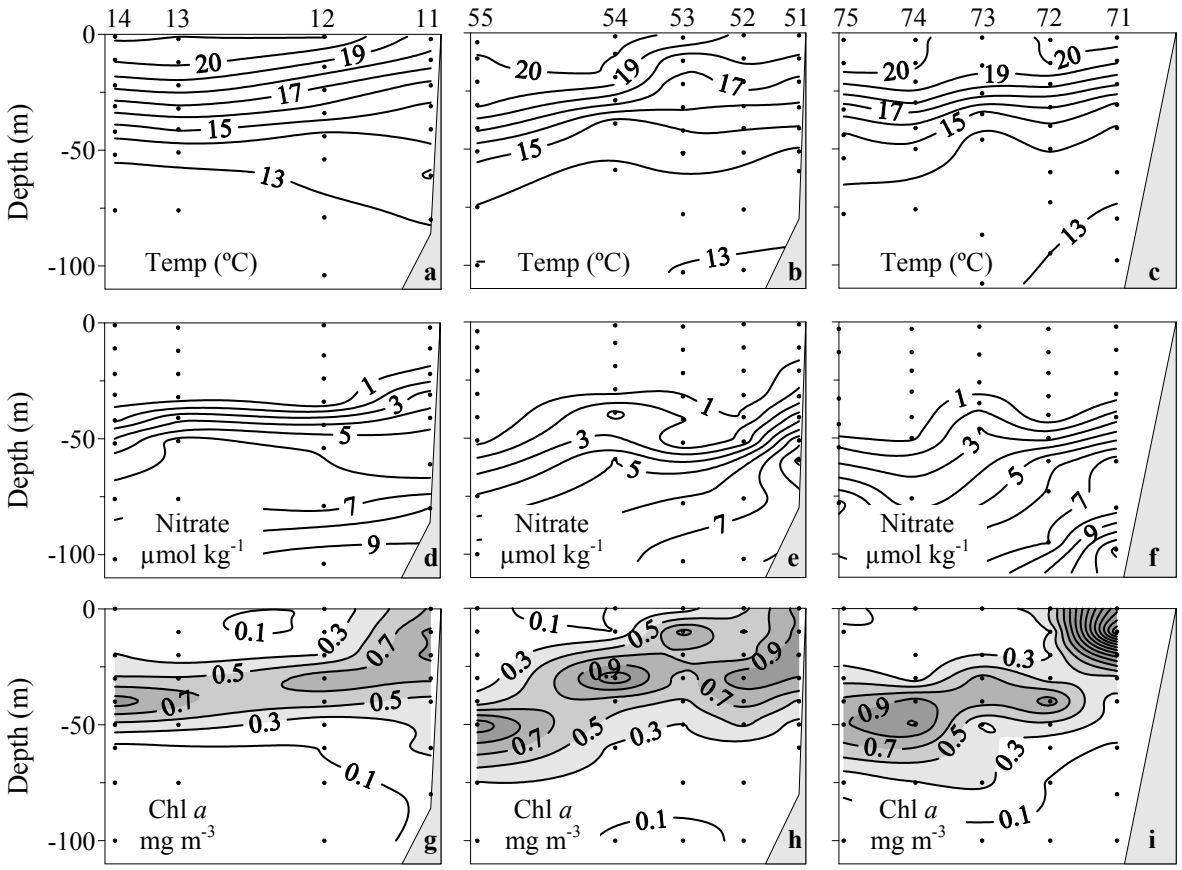

Fig. 3
Crespo et al.

Figure4
Click here to download Figure(s): Fig4.pdf

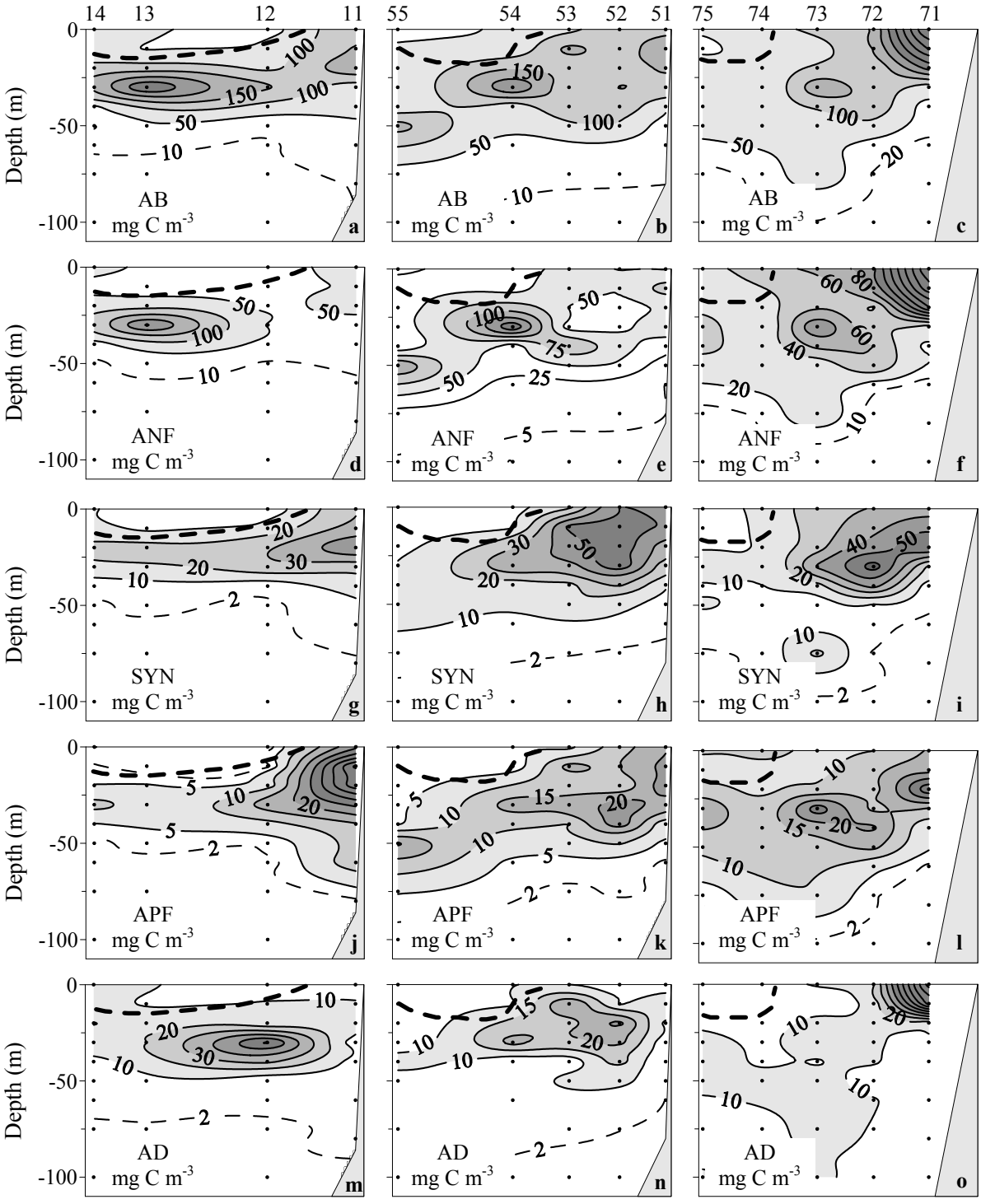

Fig. 4
Crespo et al.

Figure5

Click here to download Figure(s): Fig5.pdf

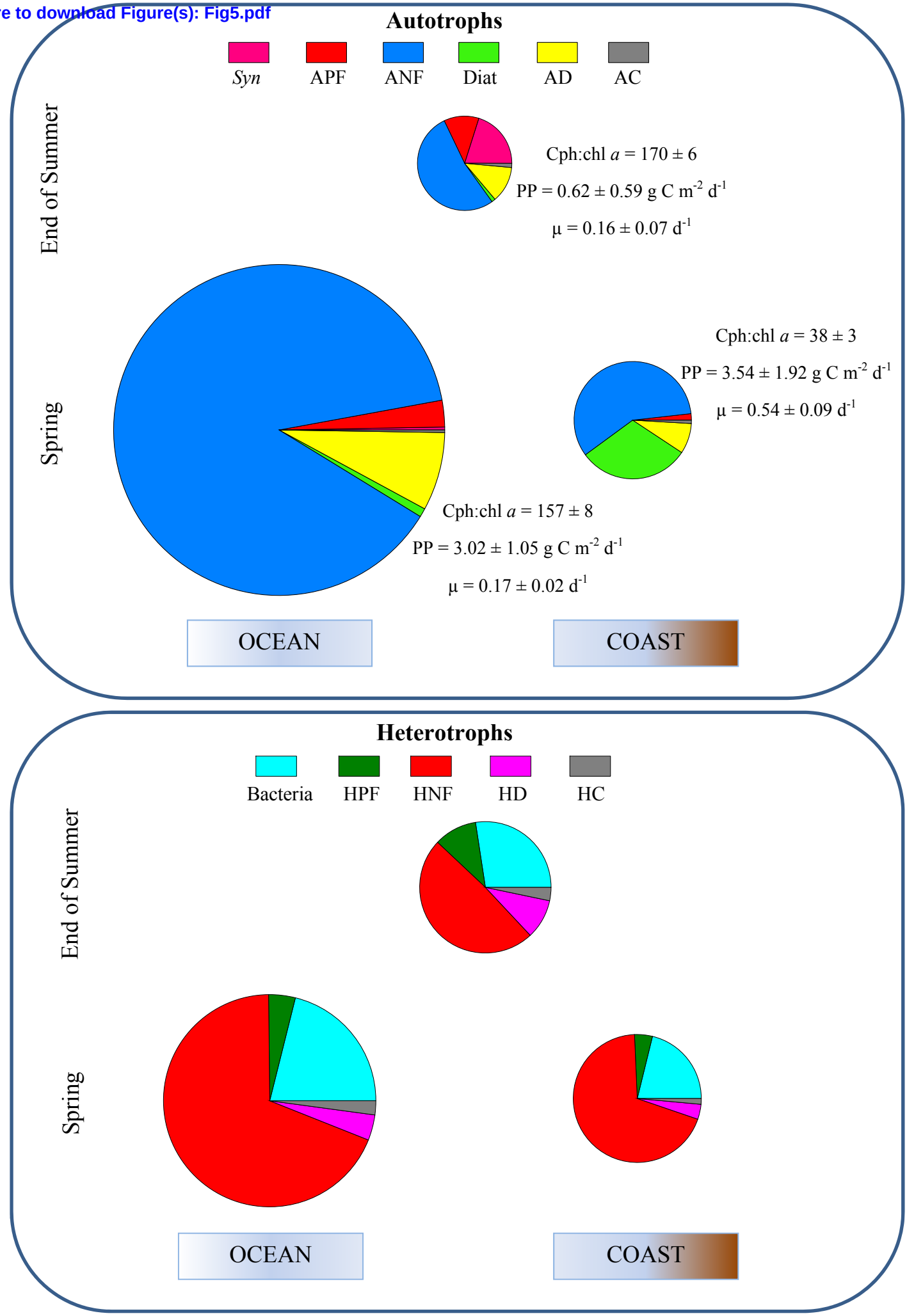

Fig. 5
Crespo et al.

Figure6
Click here to download Figure(s): Fig6.pdf

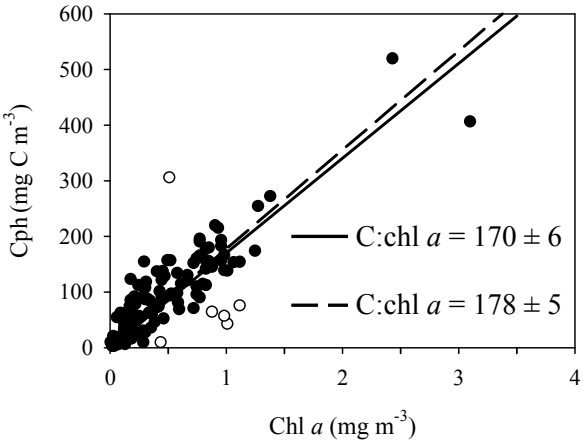

Fig. 6
Crespo et al.

Figure7
Click here to download Figure(s): Fig7.pdf

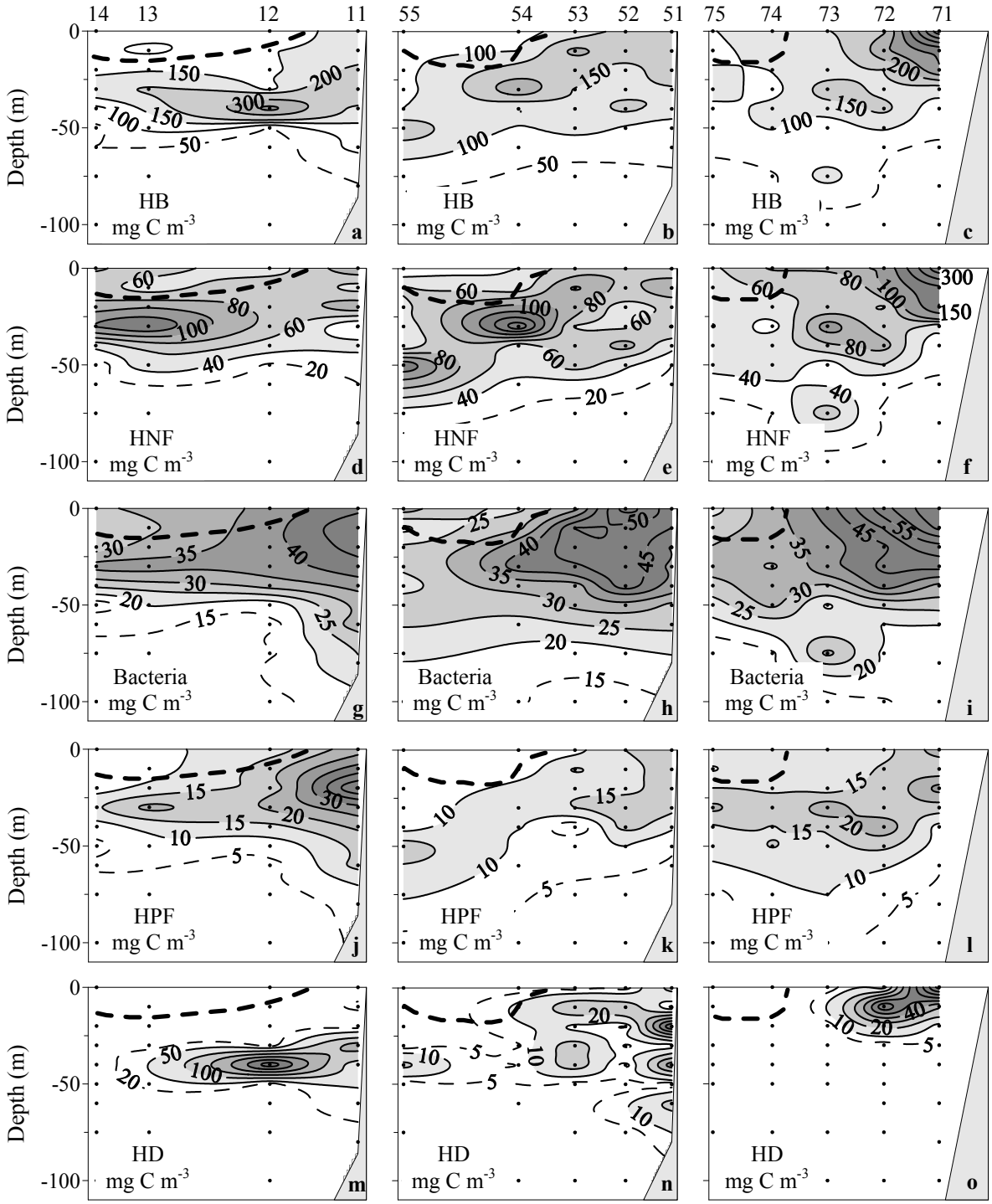

Fig. 7
Crespo et al.

Figure8
Click here to download Figure(s): Fig8.pdf

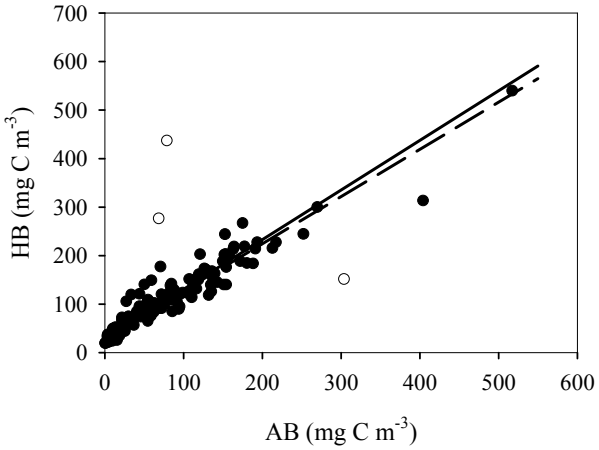

Fig. 8
Crespo et al.